Aggregation of Retail Stores

Team Members: Shahil Rais, Jared Roberts, and Matthew Rounds

Project Description

- The main objective is to understand retail store aggregation.
- Aggregation can be beneficial or detrimental towards a business attaining maximum profits.
- The profit function ultimately decides where a business will locate.

Potential Applications

- A business can utilize this model to decide where to locate their new store based on the sole criteria of maximizing profits.

Retail Store Profit Function

$$P(N_s)_s = \frac{(p_s(N_s) - p_0)D_s(N_s)}{N_s}$$

N_s = Number of stores per site.

$p_s(N_s)$ = Retail price as a function of the number of stores.

p_0 = Cost of product to the business.

$D_s(N_s)$ = Demand as a function of the number of stores.

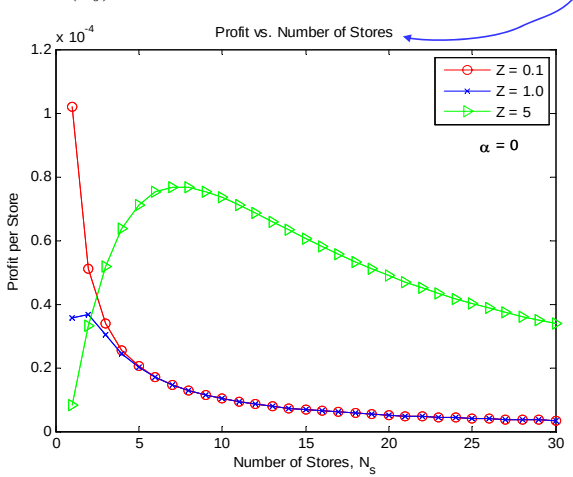

Profit vs. Number of Stores with varying Z (measure of store overlap) of a site, with utility $R = 1$ and $\alpha = 0$. The demand area is a circle.

Methodology

1. Determine the profit function for a given business.
   a) Model 1
      - The utility $R(N_s)_j$, satisfaction probability $V_s(N_s)$, travel cost $C(r_j, r_s)$, and retail price $p_s(N_s)$ are included in the demand.
      - The demand is proportional to the area of a circle which represents the region of influence for each site.
   b) Model 2
      - The demand is based on a square lattice roadway structure and is proportional to the area of a diamond.
      - The retail price $p_s(N_s)$ is modified to reflect a more realistic profit model.
   c) Model 3
      - Corresponds to Model 2 with the effect of internet included.
      - Risk Probability replaces Satisfaction Probability and Wait Time replaces the Travel Cost.
2. As aggregation intensifies, the profit of a business can either increase or decrease depending on the type of business.
3. Analyze the profit function for the effect of price competition α and the extent of product overlap Z.

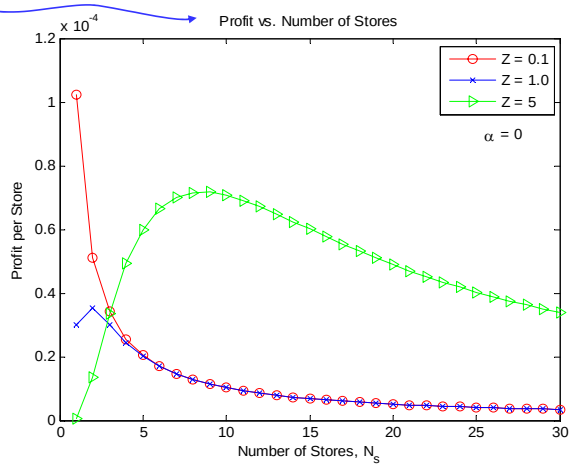

Profit vs. Number of Stores with varying Z (measure of store overlap) of a site, with utility $R = 1$ and $\alpha = 0$. The demand area is a diamond.

Glossary of Technical Terms

Site: A region where a consumer considers the distance traveled to all stores in that region to be approximately the same.

Demand: The number of consumers expected to patronize a site.

Aggregation: Businesses that are close in proximity to their competition.

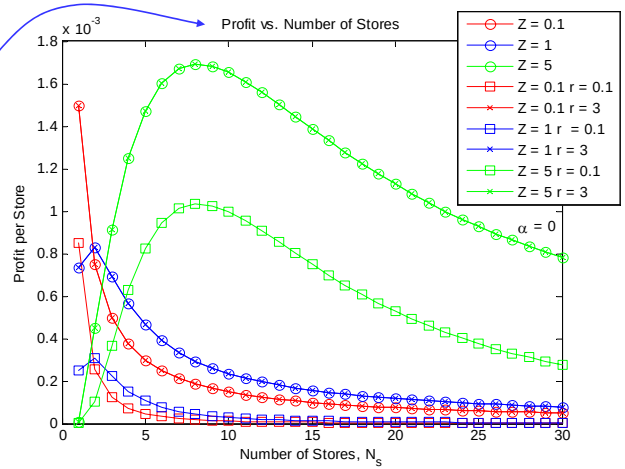

Profit vs. Number of Stores with varying Z (measure of store overlap) of a site, with utility $R = 3$ and $\alpha = 0$. The demand area is a diamond and the internet is included.

Results

1. All three models indicate that aggregation must occur if Z (measure of store overlap) is high.
2. All three models indicate that aggregation should not occur if Z is low.
3. Model 1, Model 2
   a) For $Z = 5$, Model 1 shows a maximum profit at 7 stores, while Model 2 shows a maximum profit at 9 stores.
   b) For low Z values, Model 1 and Model 2 exhibit the same non-aggregate behavior.
4. Model 3
   a) The internet factor does not affect aggregation.
   b) The internet factor decreases profits for retail stores because they do not competitively interact with internet businesses.

References

1. Jensen, Boisson and Larralde. "Aggregation of retail stores", Physica A: Statistical and Theoretical Physics 351. 2-4 (2005) : 551-5700
2. Rais, Roberts and Rounds. "Aggregation of Retail Stores", Unpublished. University of Arizona for Mathematics 485 course, Tucson, Arizona March 23, 2006.

Acknowledgments

This project was administered by Dr. Joceline Lega and mentored by Assane Lo, whose help is acknowledged with great appreciation.

Barchan Sand Dunes

Jae Anderson Luke Diaz Sujoy Ganguly Jesse Horner Shawn Miller

Project Description

- Understand and describe the fundamental mechanisms of barchan sand dune topography evolution and formation.
- Solve a one-dimensional continuous model using equations from fluid mechanics that embody physical conservation laws.

Potential Applications

- This is important because of the following applications:
  - Green House Effect and how rising sea levels influence the sand levels on beaches. This in turn effects coastal planning.
  - Understanding the climate in specific regions, and the climate characteristics that those regions have. For example, the Martian climate.

Introduction

- Barchan sand dunes form from:
  - Unidirectional Wind
  - Isolated large volumes of sand with relatively small depth
  - An initial non flat surface profile

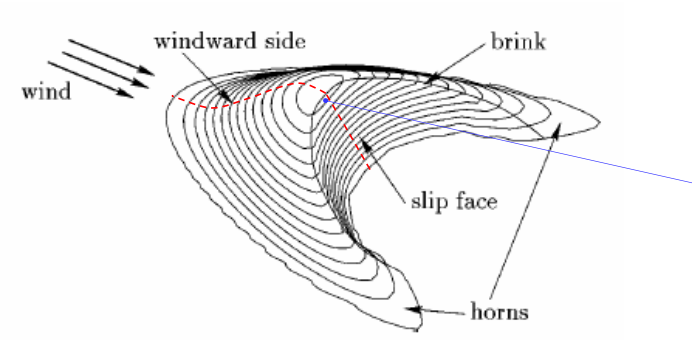

Characteristics of a Barchan sand dune with unidirectional wind (taken from [2]).

Methodology

1. The layer of sand in motion, called the saltation layer, will be treated as a fluid. The behavior of the saltation layer is governed by the shear stress caused by the wind above it, and the friction with the immobile sand bed below.
2. The initial non-flat surface profile of the sand bed will be consider as a small perturbation from a flat surface.
3. An equation for the shear stress caused by this small perturbation from a flat surface is derived.
4. An equation for the saltation flux is derived, which depends on the shear stress.
5. An equation for the change in height due to the saltation flux is also derived.
6. A numeric solution for the height as a function of time and space is found.

Results

1. Starting with two initial perturbations, the height evolution of the dune over a period of a minute is calculated.
2. The initial shear stress is calculated, the three key features are:
   1. The asymmetry of the shear stress, causes the deposition of sand.
   2. The dips of the shear stress value below the asymptotic value on either side of the dune cause a change in the slope on their respective side of the dune.
   3. The windward shift of the peak shear stress causes the deposition of sand on the top of the dune. This in turn leads to the formation of the brink.
3. As time evolves the formation of the brink causes a discontinuity in the first derivative of the height profile. This means that the numeric implementation used becomes unstable.

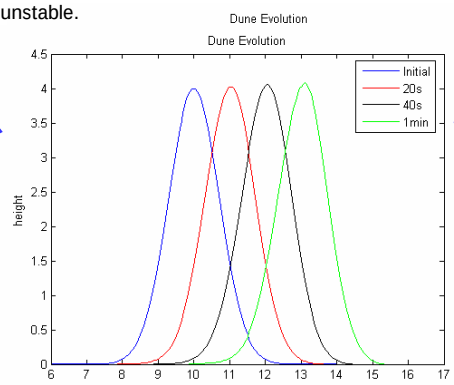

The change in height profile over a minute for a Gaussian initial perturbation.

Glossary of Technical Terms

• Shear stress: Force per unit area that is directed along the tangent plane of the surface.
• Shear velocity: A measure of the shear stress on the surface induced by the wind.
• Saltation flux: Mass of saltation layer per unit area per unit time "passing through" a vertical cross section.

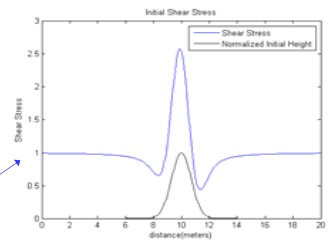

Initial height profile of dune (bottom), and corresponding initial shear stress (top).

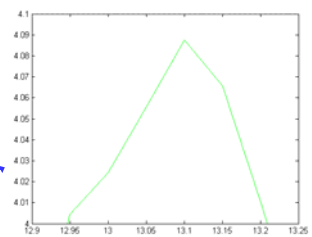

Magnification of the top of the height profile after 1 minute.

References

1. K. Kroy, G. Sauermann, H.J. Herrmann, Minimal Model for Sand Dunes, Physical Review Letters, **88**, (2002).
2. G. Sauermann, K. Kroy, H.J. Herrmann, Continuum Model For Sand Dunes, Physical Review E, **64**, 9 (2001).
3. Pye, K. Tsoar, H., *Aeolian Sand and Sand Dunes*, Unwin Hyman Ltd., (London, 1990).

Acknowledgments

This project was mentored by Eric Forgoston, whose help is acknowledged with great appreciation. We also would like to acknowledge Joceline Lega for her guidance and support.

Investigation of Borehole Reflection Tomography

Mehmet Serkan Arca, Ph.D. student, Department of Geosciences, The University of Arizona, Tucson, AZ, 85721

Introduction

• In this study, inverse methods are applied to a one-dimensional seismic borehole reflection tomography problem.
• The model simulates an experiment in which a vertical borehole is drilled through horizontal layers and seismic waves are induced, either by dynamite explosion or *vibroseis*, at some point on the surface or in the borehole. Geophones (receivers) are located at various positions in the borehole and seismic waves are recorded [1].
• The resulting data can be used to investigate layer thicknesses, seismic velocities, and ray paths. Then, the inverse problem is to determine the variation of the seismic velocity in each layer where the layer thicknesses and travel times of rays with known paths through the column are given.
• Variations of seismic velocities in each layer of the earth are important in oil exploration studies.

Definition of the Problem

• The geometry for the problem used to generate data is illustrated in Figure 1.
• The layer thicknesses (h_i) and velocities (v_i) remain constant for all scenarios, whereas sources and receivers are moved somehow arbitrarily up and down the borehole to generate different travel times.
• The horizontal component of the travel path, compared to its vertical component is neglected so that the paths are assumed to be vertical.
• The locations of the source and receiver in Figure 1 are shown for illustration purposes and the numerical values shown in Figure 1 will be used to apply for least squares method. This method will be discussed in detail.

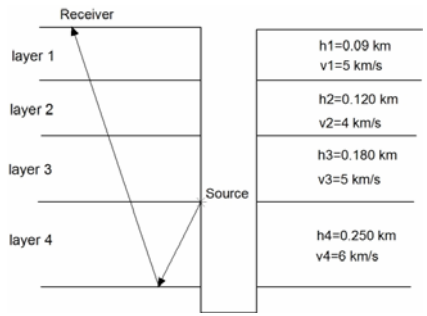

Figure 1. Borehole reflection geometry (Not to scale)

Methodology

• This problem can be used for academic investigation since the forward problem is mathematically simple and may be modeled with both linear and non-linear equations.
• The least squares method will be used in this problem. For this study, the FORTRAN program called *ginv* has been used for all calculations.

Linear Approach

Travel time is the sum of the distance traveled in each layer times the slowness of the layer, where the slowness is the reciprocal of the seismic velocity. The total travel time from source to receiver, t, is thus given by

$$t = \sum_{i=1}^{k} d_i s_i ,$$

where k is the number of horizontal layers, d_i is the distance traveled in the i^{th} layer, and s_i is the slowness of the layer material. Thus, if a ray travels through a layer on both its down-going and up-going paths, the value for d will be twice the layer thickness. In the standard form, **Gm**=**d**, the **G** matrix is composed of travel distances per layer, the **m** vector contains layer slownesses, and entries in **d** are travel times for each observation.

Least Squares Method

In order to apply inverse methods, a model that contains four layers is generated. The data that have been generated for this data set contain 10 observations (**N**=10), and four model parameters (**M**=4) so as to create a least square environment. In this method, a unique solution is expected that perfectly resolves all model parameters but has imperfect data resolution that means data cannot be fit exactly [2]. The locations of sources and receivers in the borehole and travel times for each observation are listed in Table 1.

Observation #	Source depth (m)	Receiver depth (m)	Travel time (ms)
1	390	0	167.3
2	210	0	203.3
3	90	0	233.3
4	0	0	251.3
5	640	0	125.7
6	390	90	149.3
7	210	90	185.3
8	90	90	215.3
9	210	210	155.3
10	390	210	119.3

Table 1: Data for least squares method (**M**<**N**)

Glossary of Technical Terms

Vibroseis: The most common non-explosive source used for reflection surveying. It uses truck-mounted vibrators to pass into the ground and extended vibration of low amplitude and continuously varying frequency, known as *sweep signal.*

Adding noise to the data

In order to test the stability and resolving power of the least squares solutions, Gaussian noise with a target mean value of zero and variance of 10 is generated and added to the data. The variance is chosen based on the assumption that noise in a realistic data set might have a standard deviation equal to approximately five percent of the largest data value. The noise vector generated has a calculated mean of 0.53882 and variance of 9.617669.

Observation #	Source depth (m)	Receiver depth (m)	Travel time (ms)	Noise
1	390	0	171.8	4.5247
2	210	0	204.8	1.5032
3	90	0	232.0	-1.2600
4	0	0	248.4	-2.9494
5	640	0	131.3	5.6332
6	390	90	145.3	-4.0192
7	210	90	183.5	-1.8338
8	90	90	216.0	0.7443
9	210	210	156.8	1.4847
10	390	210	120.9	1.5605

Table 2: Noisy data for least squares environment (**M**<**N**)

$$m_g = \begin{matrix} 0.217825 \\ 0.236361 \\ 0.199505 \\ 0.169264 \end{matrix}$$

$$m_{true} = \begin{matrix} 0.200080 \\ 0.250000 \\ 0.200007 \\ 0.166593 \end{matrix}$$

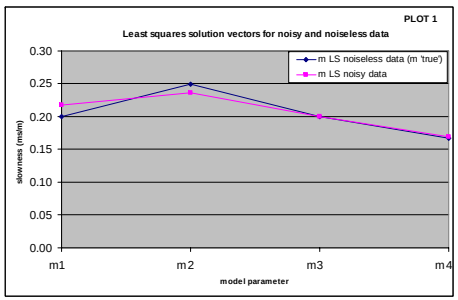

Plot 1 is a plot of the least squares solution obtained using noisy data vs. the true solution.

Conclusion

• In a situation similar to this, where investigators have the ability to determine the location and timing of events, careful forethought in designing the experiment can lead to more highly resolved and stable inverse problems.

• As far as this project is concerned, source and receivers were moved up and down the borehole with no consideration given to producing worthwhile observations. Moreover, measurements of arrivals with more complex ray paths through the column would indeed add richness and complexity to the problem.

• Finally, by using inverse methods, variations of velocities beneath the surface of the earth can be used to determine the fluid content of each layer, such as petroleum.

References

1. Kearey, P., Brooks, M., Hill, I., 2002. An Introduction to Geophysical Exploration, Blackwell Science, Third edition, 262p.
2. Menke, W. (1989), Geophysical Data Analysis - Discrete Inverse Theory, Academic Press, New York.

Mathematical Model of Tumor Metabolism

by Ajit Divakaruni

Project Overview

- **Here we present a mathematical model of the Crabtree Effect**
  - Hypoxia (low pO_2) has deleterious effects in many cancer treatments and stimulates tumor cell proliferation. Increasing oxygen concentration by decreasing consumption is an efficient, attractive therapeutic strategy [1].
  - Oxygen is consumed through cellular metabolism, which is composed of both an aerobic and an anaerobic pathway (below). Many tumors exhibit a decrease in oxygen consumption stimulated by increased glucose concentration (Crabtree Effect).

Scientific Challenges/Applications of the Model

- Although the Crabtree Effect has been established experimentally for several decades, there is a remarkable dearth of published mathematical models which show this behavior.
- Such a model, however, could prove very valuable in improving the efficacy of cancer treatment with few side effects. As opposed to many pharmacological treatments, glucose is a safe way to clinically reduce tumor hypoxia. This model is therefore essential to guide such treatments.

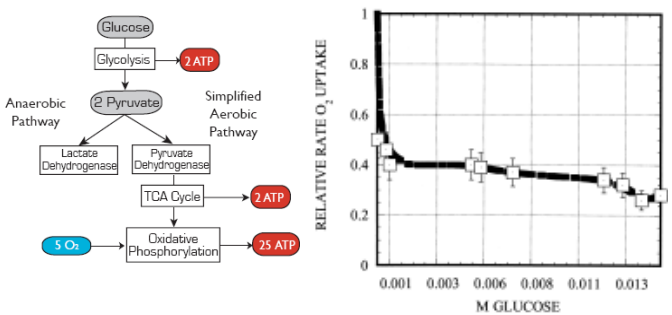

Left – A schematic representation of ATP (cellular energy) production in metabolism. The anaerobic pathway is vastly less efficient than the aerobic pathway, but can operate much faster than the aerobic pathway under tumorigenic conditions.
Right - Snyder, *et al* [2] have shown the decrease in oxygen consumption by an increase in glucose concentration (Crabtree Effect) in the R3230AC tumor cell line.

Glossary of Technical Terms

Glycolysis: The initial metabolic pathway, it produces ATP without using oxygen as a substrate. One mole of glucose is consumed for every 2 moles of ATP.
Oxidative Phosphorylation: The component of the pathway in which oxygen consumption is coupled to efficient ATP production (29 ATP per mole of glucose).
Crabtree Effect: The inhibition of oxidative phosphorylation by glycolysis. Operationally, this is seen as a decrease in oxygen consumption stimulated by an increase in glucose concentration.

Development of the Model

- Using a combination of Michaelis-Menten and mass-action kinetics, we simplified each of the major metabolic pathways.
- We distinguish between normal and tumor metabolism with a change of parameters.
  - Tumors have an increased capacity for anaerobic metabolism, the parameters V_{Gly}, K_{Gly},V_{LDH} and K_{LDH} (V_{max}'s and K_m's in Michaelis-Menten fluxes) are all increased in our simulation of tumor metabolism.
- In tumor cells, the capacity for increased ATP production by the anaerobic pathway should cause decreased ATP production from the aerobic pathway. This should decrease oxygen consumption, thereby increasing concentration.

Methodology

- Using Mathematica [3], we found numerical solutions to our system of equations governing cellular bioenergetics.

Results

- Our results indicate the system of equations is suitable to model the Crabtree Effect, though our parameters may need to be adjusted.
- As a function of increasing glucose concentration, the anaerobic pathway is better able to meet ATP demand in tumor cells relative to normal cells (below). This causes a marked decrease in oxygen consumption as glucose concentration increases (right).

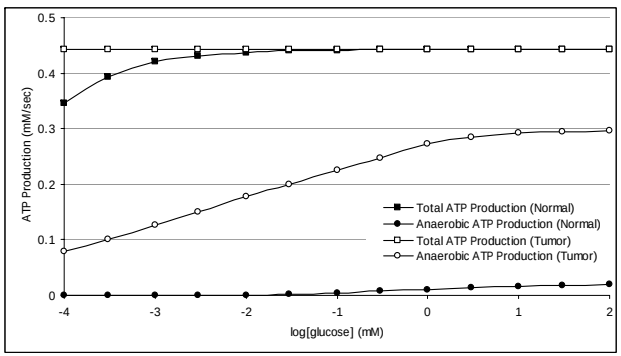

At physiologically relevant glucose concentrations (1-10 mM [2]), ATP demand is met in both normal and tumor cells. In tumor cells, however, a greater percentage of ATP is produced from the anaerobic pathway. An increase in glucose concentration stimulates even more anaerobic ATP production, subsequently decreasing aerobic ATP production.

Governing Equations for Cellular Bionergetics

$$\frac{d[Glucose]}{dt} = -\tfrac{1}{2} J_{Glycolysis}$$
$$\frac{d[Pyruvate]}{dt} = J_{Glycolysis} - J_{LDH} - J_{PDH}$$
$$\frac{d[NAD^+]}{dt} = -J_{Glycolysis} - J_{PDH} - 3J_{TCA} + 2J_{OxPhos} + J_{LDH}$$
$$\frac{d[NADH]}{dt} = J_{Glycolysis} + J_{PDH} + 3J_{TCA} - 2J_{OxPhos} - J_{LDH}$$
$$\frac{d[ADP]}{dt} = -J_{Glycolysis} - J_{TCA} - 5J_{OxPhos} + J_{ATPase}$$
$$\frac{d[ATP]}{dt} = J_{Glycolysis} + J_{TCA} + 5J_{OxPhos} - J_{ATPase}$$
$$\frac{d[Lactate]}{dt} = J_{LDH}$$
$$\frac{d[O_2]}{dt} = -J_{OxPhos}$$
$$\frac{d[AcetylCoA]}{dt} = J_{PDH} - J_{TCA}$$

$$J_{Gly} = \frac{V_{Gly}[Glu]^{1/2}[ADP][NAD^+]}{K_{Gly} + [Glu]^{1/2}[ADP][NAD^+]}$$
$$J_{LDH} = \frac{V_{LDH}[Pyruvate][NADH]}{K_{LDH} + [Pyruvate][NADH]}$$
$$J_{PDH} = \frac{V_{PDH}[Pyruvate][NAD^+]}{K_{PDH} + [Pyruvate][NAD^+]}$$
$$J_{TCA} = k_{TCA}[AcetylCoA][NAD^+]^3[ADP]$$
$$J_{OxPhos} = k_{OxPhos}[NADH]^2[O_2][ADP]^5$$
$$J_{ATPase} = \frac{V_{ATPase}[ATP]}{K_{ATPase} + [ATP]}$$

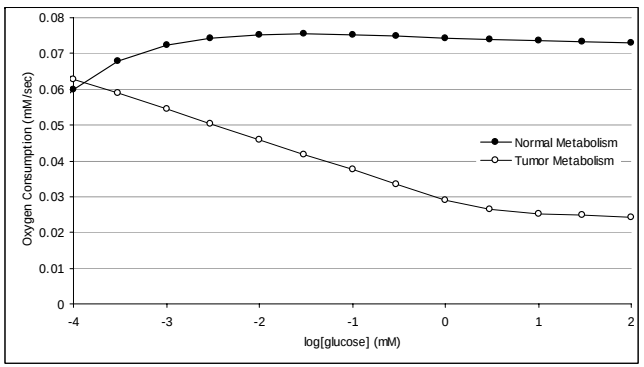

As glucose concentration increases, the increase in anaerobic ATP production in tumor cells causes a decrease in aerobic ATP production, thereby decreasing oxygen consumption (Crabtree Effect).

References

1. Snyder, SA *et al*, *Simultaneous administration of glucose and hyperoxic gas achieves greater improvement in tumor oxygenation than hyperoxic gas alone* , Int. J. Radiat. Oncol. Biol. Phys. **51(2)**, 494-506 (2001).
2. Secomb, TW *et al*, *Analysis of the effects of oxygen supply and demand on hypoxic fraction in tumors*, Acta Oncol. **34(3)**, 313-316 (1995).
3. Wolfram Research, Inc., Mathematica, Version 5.2, Champaign, IL (2005).

Acknowledgments

This project was mentored by Dr. Timothy W. Secomb, whose help is acknowledged with great appreciation.

Modeling Collective Behavior of Organisms

Project Description

- Aggregating animal behavior is often vital to a species' survival.
- Animals form groups to gain individual benefits in the forms of enhanced nutrition, reproduction, protection, and learned experience [3].
- Collective behavior is modeled by giving a simulated animal rules that govern its direction of travel determined by intelligence and neighbors [1].
- We present a computer-simulated model that generates collective behavioral patterns and studies the natural biological tendencies governing these group dynamics.

Scientific Challenges

- The exact sources of observed aggregation are unknown. Developing a model allows one to control the behavior and compare the results to those observed in the real world.
- Graphically modeling these behaviors and quantitatively tracking their individual movement leads to an understanding of the microscopic and macroscopic features of a group.
- Collective behavior is observed differently in many species like birds, fish, bees, and wild horses. This model considers groups' generic properties that have potential relevance to all aggregating species.

Potential Applications

- By manipulating simulation parameters, the probability of survival of a given aggregation characteristic can be predicted.
- Over the past decade, the animation industry has developed strategies to present more realistic cartoons using computer simulated flocking models.
- The ability to observe the flocking patterns of creatures with artificial intelligence could be useful in the future deployments of robots and emergency vehicles.

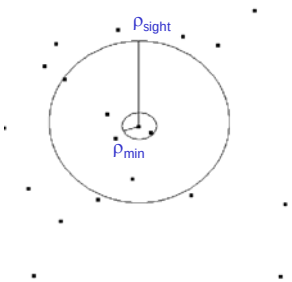

Figure 1. Two radii defining area of interaction with one's neighbors.

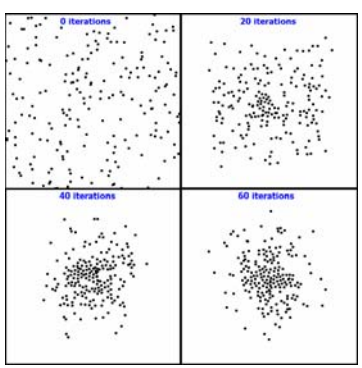

Figure 2. The collapse of a group of 200 individuals over 60 timestep iterations.

Team Members:

Caitlin Casey
Jared Jackson
Gabriel Marcus
Andrew Puza
Adam Rosenthal

A school of fish [3], and the same circular pattern seen in the simulation.

Methodology

1. The simulated animals determine their direction of travel depending on their neighbors located within radial distances ρ_{min} and ρ_{sight} (see figure 1) and on environmental information.

2. We assume the individuals' highest priority is to maintain personal space [1]. If other animals are within $\rho < \rho_{min}$ the direction vector is:

$$\vec{d}_i(t+\Delta t) = -\sum_{j\neq i}^{N_{min}} \frac{\vec{c}_j(t)-\vec{c}_i(t)}{\left|\vec{c}_j(t)-\vec{c}_i(t)\right|} \qquad (1)$$

where the vectors ***c*** and ***v*** represent the positions and velocities of the i^{th} and j^{th} animals respectively. If the individual does not detect an animal within ρ_{min} but detects animals within ρ_{sight}, the direction vector becomes:

$$\vec{d}_i(t+\Delta t) = \sum_{j\neq i}^{N_{sight}} \frac{\vec{c}_j(t)-\vec{c}_i(t)}{\left|\vec{c}_j(t)-\vec{c}_i(t)\right|} + \sum_{j=1}^{N_{sight}} \frac{\vec{v}_j(t)}{\left|\vec{v}_j(t)\right|} \qquad (2)$$

3. These animals can posses intelligence that allows them to balance their direction vector (defined in 2) with an environmental information vector.

4. To quantitatively measure group behavior, we consider three quantities: polarization, angular momentum, and group accuracy.

5. Over time, the group fluctuates in size, density, orientation, and apparent speed.

Results

1. Without intelligence, the evolution of a group shows high polarization, and very low angular momentum. This means the group's motion is highly linear without environmental or presupposed influences.

2. Group Accuracy peaks at higher fractions of an informed population, but unlike Couzin's results, an additional high correlation at low fractions is seen. From result (1) it can be gathered that at low intelligence strong polarization is seen, and this would lead to equally strong group accuracy for low intelligence.

3. Qualitatively, behavior of the animals can be manipulated to resemble circulation of fish or migration of birds.

Glossary of Technical Terms

Informed Fraction of Population: The fraction of individuals who are given full intelligence, i.e. their behavior is independent of the group.
Polarization: Indication of how individuals are aligned with each other, 0 represents no apparent group alignment and 1 represents complete alignment [2].
Angular Momentum: Measure of the circulation of the group about its center of mass, also ranging from 0 to 1 [2].
Group Accuracy: The tendency of individual alignment with the rest of the group over 50 timesteps. This differs from polarization, which is an instantaneous measurement [1].

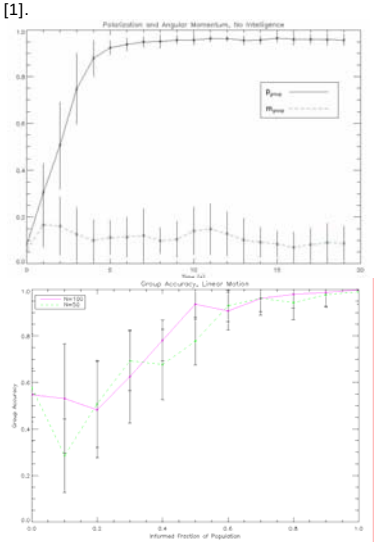

Figure 3 (top) shows the strong polarization over time in a group with no intelligence. In Figure 4 (above), the correlation between group accuracy and fraction of informed individuals is seen. Two group sizes are sampled. Figures 3 and 4 were compiled using IDL [5].

References

1. Couzin, I.D., Krause, J., Franks, N.R. & Levin, S. Effective leadership and decision making in animal groups on the move. Nature. 433, 513-516 (2005).
2. Couzin, I.D., Krause, J., James, R., Ruxton, G.D. & Franks, N. R. Collective memory and spatial sorting in animal groups. J. Theor. Biol. 218. 1-11 (2002).
3. Parrish, Julia K. & Edelstein-Keshet, Lisa. Complexity, Patterns and Evolutionary Trade-offs in Animal Aggregation. Science, 284, 99-101 (1999).
4. Animation Library. (1992) Doug Toussaint, Physics Department, University of Arizona.
5. IDL Version 6.1.1, Mac OS X (darwin ppc m32). © 2004, Research Systems, Inc.

Acknowledgments

This project was mentored by Tom LaGatta, whose help is acknowledged with great appreciation.

Modeling dislocations in an elastic half-space

Sarah K. Thompson

Project Description

In order to mitigate the earthquake hazards, understanding the deformation resulting from various types of ground displacements is essential. Earthquakes release part of the stress accumulated within the Earth due to the driving force of plate tectonics. Between earthquakes stress builds up until the material can no longer support the force, thereby undergoing brittle failure in yet again. This is known as the earthquake cycle. Understanding where the stress conditions lie within this cycle is inherent for understanding the likelihood of earthquake occurrence, as earthquakes can be triggered by stress changes. For this reason, it is important to understand Earth deformation processes.

This modeling project uses the analytic expressions described in compact form by Okada (1985) to study the surface displacement field due to three different fault rupture, *or* dislocation, scenarios in an elastic half-space:

1. Strike-slip
2. Thrust fault
3. Tensile fault

Methodology

1. The displacement field, $u_i(x_1, x_2, x_3)$, due to a dislocation $du_j(x_1, x_2, x_3,)$ across a surface S is given by:

$$u_i = \frac{1}{F}\int_z \int \Delta u_j \left[\lambda \delta_{jk} \frac{\partial u_i^n}{\partial \xi_n} + \mu \left(\frac{\partial u_i^j}{\partial \xi_k} + \frac{\partial u_i^k}{\partial \xi_j} \right) \right] \nu_k d\Sigma \qquad \textit{(Okada, 1985)}$$

   Where we assume the material is a Poisson solid.

2. Okada (1985) developed compact analytic expressions for the surface displacement field due to a dislocation on a rectangular fault. Using the Okada Fortran code, and passing in the parameters listed before using MATLAB, the surface displacements are calculated at specified "observation" points.

3. Parameters:
   L: Length of fault 50km
   W: = Width of fault in dip direction 40km
   Type: Strike-slip, thrust, or tensile
   Dip angle: counter-clockwise, form horizontal
   strike-slip, tensile: $\delta = 90°$
   thrust fault: $\delta = 45°$
   Slip: The magnitude of dislocation occurring on the center of the fault tile: S = 1 m
   X: observation points at surface; displacements are calculated every 10 km for 50 km in each direction from the midpoint of the fault.

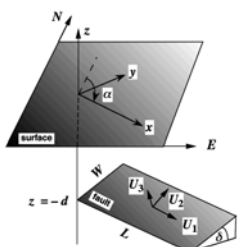

Figure 1: Illustration of geometrical parameters. The displacements due to a dislocation, **U**, along a fault of length L and width W are calculated at the surface. $\mathbf{U_1}$ corresponds to strike-slip motion; $\mathbf{U_2}$ corresponds to thrust- or reverse thrust-fault motion; and slip in the $\mathbf{U_3}$ direction corresponds to tensile deformation (i.e. inflation of a volcano due to the accumulation of magma).

Results

Using the analytical expressions for surface displacement due to a dislocation on a finite rectangular fault (Okada 1958), the displacement field due to 1m of slip the three fault geometries described is modeled. The first set of plots below shows the displacement field associated with each fault type. Each displacement field is further broken down its their x, y, and z components (*see colored plots, below*).

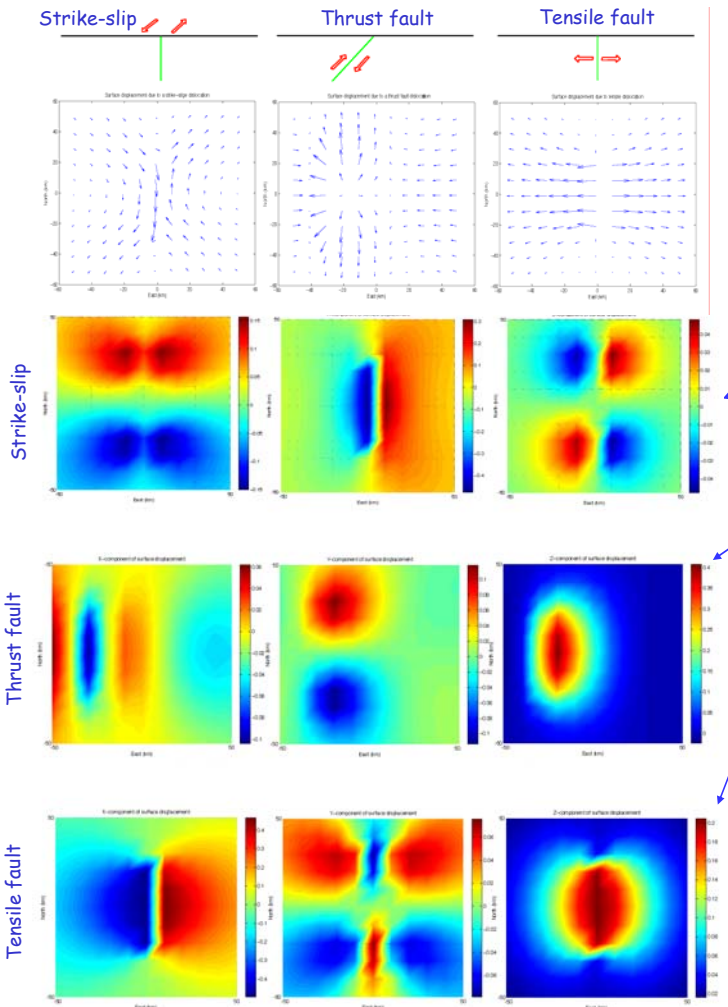

Glossary of Technical Terms

Dislocation: Finite slip on a fault, such as the displacement on a fault due to an earthquake.
Half-Space: Isotropic, homogeneous space bounded by one plane.
Lamé constants: The elastic constants, λ and μ. The Shear modulus, μ, or rigidity, is the stress-strain ration of a material. λ is also known as fluid incompressibility.
Poisson solid: Material where λ = μ. This is a good approximation for the Earth's crust.
Strike-slip: Fault geometry defined by two rock volumes moving past one-another, e.g. the San Andreas fault.
Tensile: Pertaining to the stress associated with the stretching of an elastic body. The inflation of a magma chamber is an example of tensile deformation.
Thrust fault: Fault geometry defined by two rock volumes converging toward one another, with one subducting beneath the other.

Conclusion

Elastic half-space dislocation modeling reproduces deformation observed at the surface with GPS data even though the theory was introduced many years prior to space geodetic techniques.

Deformation calculated in the strike-slip model shows deformation primarily in the N-S direction, with displacements as large as 0.4 m occurring near the center of the surface expression of the fault. Uplift and subsidence, shown in red and blue, respectively, are in four clearly defined quadrants, as observed in nature.

The thrust fault model shows small amounts of E-W compression at 50 km West of the fault. The greatest amount of deformation occurs in the vertical component, with 0.4 m of uplift above the thrust interface. Fault propagation folds, a geological structure with significant vertical movement, are a result of this type of thrust in nature.

The tensile dislocation example shows 0.5 m of displacement in the E-W direction, in addition to 0.2 m of uplift above the source region.

References

1. Okada, Y. *Surface deformation due to shear and tensile faults in a half-space.* Bull. of the Seismological Soc. of America **75**, 1135-1154 (1985).
2. Okada, Y. *Internal deformation due to shear and tensile faults in a half-space.* Bull. of the Seismological Soc. of America **82**, 1018-1040 (1992).
3. Steketee, J. A. *On Volterra's dislocation in a semi-infinite elastic medium*, Can.J. of Phys. **36**, 192-205 (1958).

Acknowledgments

Thanks to Dr. S. Hreinsdóttir for her assistance with this project. This work was made possible through support from the University of Arizona Department of Geosciences.

Modeling the Spread of SARS Using Small World Networks

Project Description

- Create a program that models the spread of an epidemic using small world network theory and SNIR concepts.
- Show how this model is implemented in our case study on the spread of SARS in Hong Kong.
- Illustrate how the disease spreads through social networks with non-uniform demographics, as opposed to traditional SIR models that represent the population with one demographic.

Scientific Challenges

- Scientists are seeking new methods to understand how the rate of transmission of a disease accelerates.
- With recent outbreaks of SARS, Mumps, and Influenza, more attention has been focused on the impact of small world networks in the spread of a disease.

Potential Applications

- This program could potentially be used for modeling the spread of other diseases similar to SARS such as Influenza and Tuberculosis. Demographic parameters can be altered to tailor the geographic location and the type of disease.

The flip book above illustrates what the program outputs at each time iteration. We see how small world networks work by observing the progression of people getting infected by their neighbors.

Team Members:

Tim Gonzalez, Masa Iwado, Kristie Manalo, Jason Simental, Larrison Nez

Methodology

1. We designed a Java-based program with the following input parameters:
   - 3 values representing the population for each age group.
   - 3 values representing the susceptibility of each age group to the disease.
   - 2 threshold values from our probability index.

   In each iteration, the program identifies persons susceptible to catch the disease and decides whether they become infected, based on their level of susceptibility. The program then outputs the following information:
   - Number of people who are newly infected.
   - Total number of people who are infected.
   - Total number of people who have recovered from the disease.
   - Total number of people who have died from the disease.
2. We ran many simulations for each threshold value from our probability index. We also conducted a statistical analysis with MS Excel.
3. Based on empirical demographic data from Hong Kong, we determined the optimal threshold value that reflects a realistic outbreak of SARS in Hong Kong.
4. We then compared our program's results for SARS in Hong Kong to values reported by Hong Kong's Department of Health.

Results

1. We simulated and graphed the averages of days for an epidemic as well as the number infected, and the number recovered for over 100 trials at each probability index value.
2. We found that the optimal probability index for SARS in Hong Kong based on data report in [2] is 33.
3. We created a histogram based on the data we collected by running 62 trials of the simulation for P.I.= 33. The histogram shows that the average number of people infected is 1624, which is the approximate number of people infected with SARS in Hong Kong 2003.

Glossary of Technical Terms

Small World Network: Class of random graphs which "have many vertices with sparse connections" [3] but where "every node can be reached from every other by a small number of hops or steps" [4].
SNIR: Susceptible-Newly Infected-Infected-Recovered categorization.
Probability Index (P.I.): A set of integer threshold values in the interval [5,100], which are compared to a uniformly distributed random number in order to decide whether a person becomes infected or recovers.

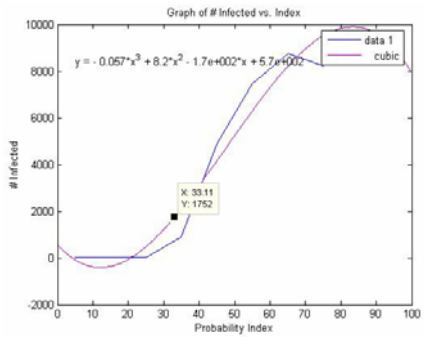

Number of infected people as a function of the probability index, fitted and plotted with MATLAB.

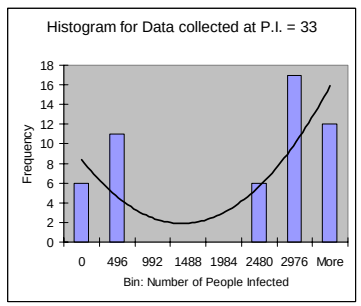

Histogram of the number of infected people for 62 different trials, with P.I. = 33

References

1. M. Small and C.K. Tse, *Clustering model for transmission of the SARS virus: application to epidemic control and risk assessment,* Physica **A 351**, 499-511 (2005).
2. G.M. Leung *et al*, *The Epidemiology of Severe Acute Respiratory Syndrome in the 2003 Hong Kong Epidemic: An Analysis of All 1755 Patients,* Ann Intern Med. **141**, 662-673 (2004).
3. D.J. Watts and S.H. Strogatz, *Collective Dynamics of 'small-world' networks*, Nature **393**, 440-442 (1998).
4. Wikipedia, *The Free Encyclopedia*.

Acknowledgments

This project was mentored by Dr. Lega, whose help is acknowledged with great appreciation.
Anya Peterson is also gratefully acknowledged.

Price Dispersion

Team Members: Christian Botsford • Christopher Caraway • Ding Shen • Emily Simpson • Gloria Yeomans

Project Description

- **Motivation**: To examine why stores charge different prices for identical goods.
- **Objective**: To model price dispersion due to transportation cost and information differences over realistic population densities.
- **Reason**: To develop a model which deals with the cost of transportation, imperfect information and different population densities.
- **Previous Works:** It has been theorized that price dispersion occurs due to imperfect information [1].

Scientific Challenges

- A realistic model to explain the direct causes of price dispersion is currently implausible due to the large number of potential variables.
- This project seeks to examine the effects of transportation cost in various population densities.

Potential Applications

- Knowledge of price dispersion would have relevance in consumer welfare, price stability, and market efficiency.

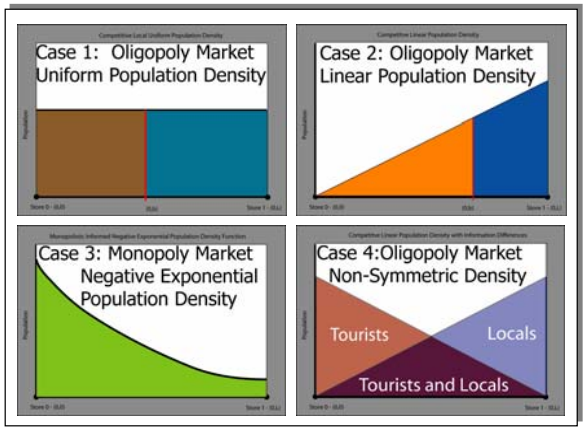

Set up

- The model considers two firms, store 0 and store 1, which charge prices P_0 and P_1. The stores can operate as either a monopoly or an oligopoly.
- Differences in the level of information among a population is represented by two types of buyers (locals and tourists) with their respective population densities, $\Phi_{locals}(x)$ and $\Phi_{tourists}(x)$.
- Each of the populations has a demand D_m and purchase a quantity $D(x) = D_m - (\gamma \cdot P_i + C_t \cdot x)$ where γ is the elasticity of the good, P_i is the cost charged by a store, and C_t is the cost of transportation.
- The locals have perfect information and purchase the cheapest good. Tourists will always purchase from the closest store.

Methodology

1. Calculate the total profit, π, for the firms where $b = \dfrac{-P_0 + P_1 + L}{2 \cdot C_t}$

$$\pi_0(P_0, P_1) = \int_0^b P_0 \cdot \Phi(x) \cdot [D_m - (\gamma \cdot P_i + C_t \cdot x)]dx$$

$$\pi_1(P_0, P_1) = \int_b^L P_1 \cdot \Phi(x) \cdot [D_m - (\gamma \cdot P_i + C_t \cdot x)]dx$$

2. Determine when the firms maximize profit

$$\left.\frac{\partial \pi_0(P_0, P_1)}{\partial P_0}\right|_{P_1} = 0 \quad \text{and} \quad \left.\frac{\partial \pi_1(P_0, P_1)}{\partial P_1}\right|_{P_0} = 0$$

Differences in market information and market type are considered when calculating the profit functions.

- For oligopoly market the profit functions π_0 and π_1 are examined individually. For a monopoly the $\pi_{monopoly} = \pi_0 + \pi_1$.
- There are two groups in every population, locals and tourists. The profit functions are added together so that the profit for one firm facing a heterogeneous population is $\pi_{population} = \pi_{locals} + \pi_{tourists}$.

3. Locate the curves in the P_0, P_1 plane that maximize π.
4. Generate a P_0 vs P_1 graph representing the market equilibrium(s).

Results

Market Description	P_0	P_1	b
Case 1: Oligopoly - Uniform Population Distribution	$0.92	$0.92	0.50
Case 2: Oligopoly - Linear Population Distribution	$0.60	$0.87	0.64
Case 3: Monopoly - Exponential Population Distribution	$4.88	$4.88	0.50
Case 4: Oligopoly - Non-Symmetric Population Distributions	**$4.83**	**$3.82**	**1.00**

- **Case 1 -** No price dispersion ($P_0 = P_1 = P$), low market price (P < $1), symmetric balance point (b = 0.50).
- **Case 2 -** Price dispersion($P_0 \neq P_1$), low market price, non-symmetric balance point (b ≠ 0.5). *This suggests that store 0 would aggressively lower prices to steal a portion of the market away from store 1.*
- **Case 3 -** No price dispersion, symmetric balance point, high market price (P > 1). *In this case the two firms maximize their profit by minimizing the cost of transportation.*
- **Case 4 -** Price dispersion, high market price, non-symmetric balance point. *This result differs from Case 1 with tourists in that the alternate equilibrium ($3.82,$4.83) has become unstable.*

Glossary of Technical Terms

Monopoly: When the production of a good or service with no close substitutes is carried out by a single firm with the market power to decide the price of its output [2].

Oligopoly: When a few firms dominate a market [2].

Demand (D_m): Amount of a good or service that people are both willing and able to buy [2].

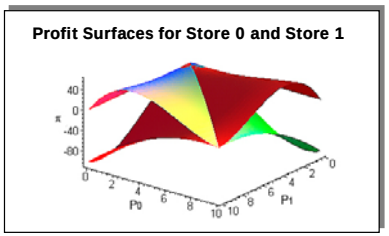

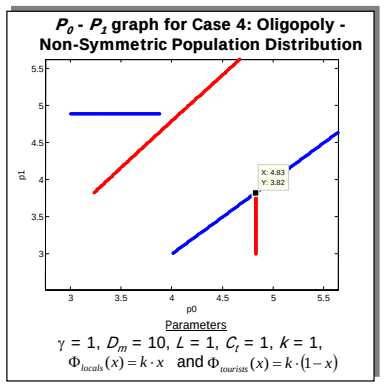

References

1. Stigler, George J. "The Economics of Information." The Journal of Political Economy 69.3 (1961): 213-225.
2. Research Tools. Economics A-Z. The Economist. May 1, 2006. <http://www.economist.com/research/Economics/>

Acknowledgments

This project was mentored by Tommy Ochippinti and J. Lega, whose help is gratefully appreciated.

Resistance to Antibiotics

Project Description

- The goal of the project is to present an accurate model of antibiotic resistance at the bacterial (host/patient) level which can be used to study treatment effects.
- Our model is based on ones previously proposed by Webb *et al* [4], Levin & Stewart [3] and Bergstrom & Lipsitch [1].
- A model is needed to study the interactions between resistant and nonresistant bacteria at the individual level.

Scientific Challenges

- Antibiotic resistance in bacteria is becoming a problem for hospitals nationwide.
- Our challenge is to present a model which represents the interactions between resistant and nonresistant bacteria within the body.

The Model

- N = number of nonresistant bacteria
- P = number of resistant bacteria
- ρ = recombination rate
- μ = reversion rate
- χ = carrying capacity
- β_n = growth rate of nonresistant bacteria
- β_p = growth rate of resistant bacteria
- n = density of nonresistant bacteria
- p = density of resistant bacteria
- h = growth rate of n
- s = spontaneous reversion rate
- g = effective growth rate of p

$$\begin{cases} \frac{dN}{dt} = \left[\beta_N N - (\frac{N}{\chi})(N+P)\right] - \left[\rho N(\frac{P}{N+P})\right] + [\mu P] \\ \frac{dP}{dt} = \left[\beta_P P - (\frac{P}{\chi})(N+P)\right] + \left[\rho N(\frac{P}{N+P})\right] - [\mu P] \end{cases}$$

growth rate
nonlinear saturation
recombination term
spontaneous reversion

$$h \equiv \frac{\beta_n}{\rho} \qquad g \equiv \frac{(\beta_n - \mu)}{\rho}$$

$$s \equiv \frac{\mu}{\rho} \qquad n \equiv \frac{N}{\rho\chi} \qquad p \equiv \frac{P}{\rho\chi}$$

$$\begin{cases} \frac{dn}{dt} = hn - n(n+p) - n(\frac{p}{n+p}) + sp \\ \frac{dp}{dt} = gp - p(n+p) + n(\frac{p}{n+p}) \end{cases}$$

Methodology

1. Rescale the model from five to three parameters.
2. Solve for critical points
3. Analyze stability of critical points based on varying parameter values
4. Verify phase-plane analysis using PPLANE [3] software

Team Members:

René Bernal-Gonzales
Matt Foster
Maaz Iqbal
Arjang Talattof
Seth Wagenman

Results

The trace and determinant of the linearized system show that the density of nonresistant bacteria can approach a stable value and persist—though at much smaller levels than the resistant strain—even when treated. For the third fixed point (inset in fig. 1) to be stable, the trace should be negative and the determinant positive. We consider these cases while varying the parameter h, and determine the values of n (on a semi-logarithmic scale) where this relationship holds true (fig. 2). The stable equilibrium indicates that by lowering, rather than completely eliminating, h (through treatment, for example), and having $\mu << \rho$, the resistant bacteria proliferate while the nonresistant are rendered nearly negligible, highlighting the competitive nature of the two strains.

$$J(n,p) = \begin{bmatrix} h - 2n - p - \frac{p^2}{(n+p)^2} & -n + s - \frac{n^2}{(n+p)^2} \\ -p + \frac{p^2}{(n+p)^2} & g - 2p - n + \frac{n^2}{(n+p)^2} \end{bmatrix}$$

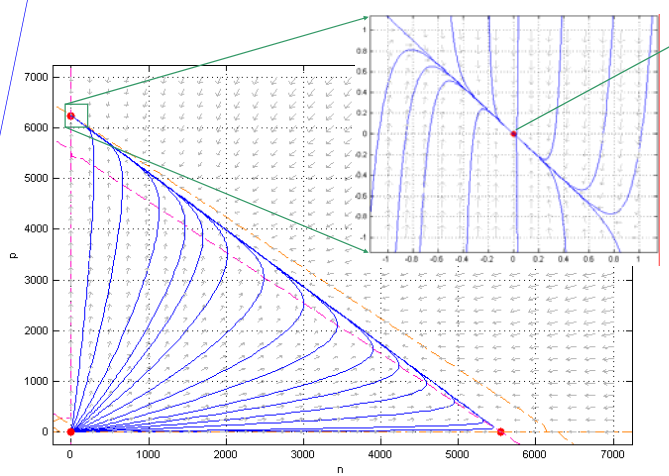

Figure 1: Phase-plane analysis using PPLANE. The n-nullclines and p-nullclines are shown in orange and red, respectively. Fixed points are found at the origin, at (5545.18,0) and (0.08987, 6238.2). Since this plot is not on a logarithmic scale, the upper-left fixed point appears to lie on the p-axis. It is actually a stable node, as seen in the inset displaying the linearization about the point.

Glossary of Technical Terms

Recombination: The transfer of DNA from one organism to another. The donor DNA may then be integrated into the recipient's genome by various mechanisms.
Reversion: The return of genetic character to the original state of the recipient. In the case of resistant bacteria, it is the return of the recipient bacteria to the non-resistant state through recombination with non-resistant bacteria. Reversion occurs through the same mechanisms as recombination. *Note*: Since the probability of recombination decreases each time it occurs, reversion is less likely to occur after the first recombination. Therefore, the rate of recombination is greater than the rate of reversion.

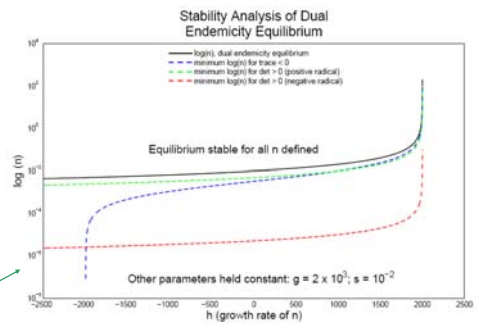

Figure 2: Matlab simulation, semi-log plots. The blue curve represents the value of log(n) above which the trace is negative; the determinant is positive above both the red and green curves; the black curve represents log(n) at the third fixed point, as a function of h. Thus the case where trace $< 0 <$ determinant at the fixed point occurs where the black function is greater than both the blue and the red/green.

References

1. Bergstrom, C.T., Lo, M. & Lipsitch, M., *A model of antibiotic resistant bacterial epidemics in hospitals*, Proc. Natl. Acad. Sci. USA **94**, 13285 – 13290 (2004).
2. Feil E.J., Spratt B.G. *Recombinatoin and the population structures of bacterial pathogens*, Annu. Rev. Microbiol. **5,** 561--90, 2001
3. Lewis, R., *The rise of antibiotic-resistant infections*, FDA Consumer **29**, 11 – 5 (1995).
4. ODE Software for MATLAB http://math.rice.edu/~dfield/
5. Stewart, F.M. & Levine, B.R., *A model of antibiotic-resistant bacterial epidemics in hospitals*. Genetics **87**, 209 – 228 (1977).
6. Webb, Glenn F., Erika M.C. D'Agata, Pierre Magal & Shigui Ruan. *A model of antibiotic-resistant bacterial epidemics in hospitals*. PNAS **102**, 13343 – 13348 (2005).

Acknowledgments

We would like to thank our mentor, Marco Herrera, whose help was invaluable. Dr. Lega is also greatly appreciated. We would also like to acknowledge Dr. Webb for providing us with his original Mathematica code for the simulations.